

## Light Guiding in Low Index Materials using High-Index-Contrast Waveguides

Vilson R. Almeida, Qianfan Xu, Roberto R. Panepucci, Carlos A. Barrios, and Michal Lipson  
Cornell University, School of Electrical and Computer Engineering, 429 Phillips Hall  
Ithaca, NY 14853, U.S.A.

### ABSTRACT

We propose a novel high-index-contrast waveguide structure capable of light strong confinement and guiding in low-refractive-index materials. The principle of operation of this structure relies on the electric field (E-field) discontinuity at the interface between high-index-contrast materials. We show that by using such a structure the E-field can be strongly confined in a 50-nm-wide low-index region with normalized average intensity of  $20 \mu\text{m}^{-2}$ . This intensity is approximately 20 times higher than that can be achieved in  $\text{SiO}_2$  with conventional rectangular or photonic crystal waveguides.

### INTRODUCTION

Recent results in integrated optics have shown the ability of efficiently guiding, filtering, bending and splitting light on chips using a variety of waveguide structures [1]. Extremely sharp curves, bends, and splitters have also been demonstrated, allowing a high level of integration [2,3]. Multiplexers and demultiplexers using resonant structures such as ring resonators have been shown [4]. All of these structures are based on total internal reflection (TIR) as the guiding mechanism. This mechanism is commonly thought to prohibit the light to be confined and guided in the lower-index region. In the last few years, guiding light in low-index materials has become increasingly important for applications such as optical sensing, interaction with low index materials, and avoiding nonlinearities in the high-index material.

Early attempts to guide light in the low-index material on high-index-contrast platform led to structures that are wavelength dependent and have relatively large transverse dimensions, which limited their optical intensity and ability for integration. The antiresonant reflecting optical waveguide (ARROW) structure uses the external reflection at the high-index-contrast interfaces as a guiding mechanism [5], in contrast to the total internal reflection used in standard waveguides; this structure was recently proposed for sensing applications [6]. Based on similar principles, the OmniGuide fibers and photonic band-gap fibers were investigated [7,8], where 1-D or 2-D periodic structures are used to provide the near-unity reflections for guiding. All aforementioned structures are wavelength dependent, inherently leaky, and present large cross sectional dimensions of at least several micrometers.

We propose a waveguide structure that can confine light inside a nanometer-wide area of low-index material with high E-field amplitude and optical intensity. In contrast to the leaky nature of the previously mentioned structures, the guided mode is an eigenmode of our proposed structure; therefore, it is fundamentally lossless. Our proposed structure, hereafter named slot-waveguide, consists of two parallel high-index contrast waveguides separated by a nanometer-sized low-refractive-index slot. Since the slot-waveguide does not rely on resonance principles, the eigenmode is almost wavelength insensitive. Furthermore, it is fully compatible with highly-

integrated photonics technology, retaining most of its important properties such as nanometer-sized cross-section dimensions and small minimum bend radius. For the quasi-TE eigenmode the slot is obtained by lithographic patterning, whereas for the quasi-TM counterpart appropriate multilayer design is requested. Potential applications for the slot-waveguide include host for active materials, sensing, non-linear optics, optical modulators and switches, near-field optical microscopy (NSOM), and efficient coupling to nanometer-sized waveguides and structures.

## THEORY

The principle of operation of the slot-waveguide is based on the discontinuity of the normal component of the E-field  $E$  at the high-index-contrast interface. From Maxwell's equations, the normal component of the electric flux density  $D$  is continuous at the interface of two dielectric materials. Since  $D = \epsilon_r \epsilon_0 E = n^2 \epsilon_0 E$ , where  $n$ ,  $\epsilon_r$  and  $\epsilon_0$  are the refractive index, dielectric constant and vacuum permittivity, respectively, the normal component of  $E$  shows discontinuity if  $n$  is different at opposite sides of the interface. The E-field is then higher at the low-index side and lower at the high-index side, with the ratio equal to the square of the index contrast  $(n_{\text{High}}/n_{\text{Low}})^2$ . This discontinuity has usually been overlooked because most of the investigated photonic structures rely on low-index-contrast. However, for high-index-contrast structures, this discontinuity is significant. For example, at the Si/SiO<sub>2</sub> interface, the normal component of E-field at the SiO<sub>2</sub> side is 6 times higher than that at the Si side. At the Si/air interface, the normal component of the E-field at the air side is 12 times higher than that at the Si side.

An example of a slot-waveguide is shown in figure 1; it consists of a low-index region embedded between two rectangular high-index regions. In such a structure, the major component of the E-field of the quasi-TE mode is in the horizontal direction, normal to the walls of the slot. Due to the high index contrast, the E-field has a discontinuity at the walls, with much higher amplitude in the slot than that in the high-index part of the structure. Due to the fact that the dimensions of the slot are comparable to the decay length of the field, the E-field amplitude will remain high over the whole region of the slot. Therefore, the average E-field amplitude in the slot becomes much higher than that in the high-index material. The optical intensity in the slot is also much higher than that in the high-index region, since the magnetic field (H-field) is continuous at the interface and varies slowly across the structure. On the other hand, the major E-field component of the quasi-TM mode is parallel to the interface of index contrast, resulting in an E-field that is continuous at the walls of the slot. As a result, the presence of the slot does not affect the quasi-TM mode as strongly as it affects the quasi-TE mode.

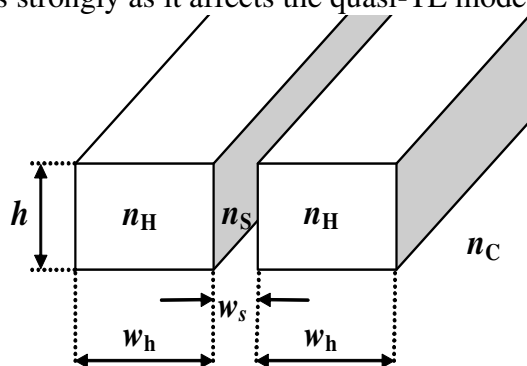


**Figure 1.** Schematic of a slot-waveguide

We numerically analyzed the performance of the structure shown in figure 1 for guiding and confining light in nanometer-size low index regions. A full-vectorial finite difference mode solver [9] with non-uniform grid mesh was implemented to simulate the quasi-TE eigenmodes of slot-waveguides with different dimensions and wavelengths. For concreteness, we assume that the slot-waveguide is built on the widely used Silicon-On-Insulator (SOI) platform, with the silicon being the high-index material, and the silicon dioxide being the low-index cladding;  $n_H = 3.48$ ,  $n_C = 1.46$ , and a wavelength of  $\lambda_0 = 1.55 \mu\text{m}$  are assumed, unless otherwise specified. We also assume that the slot is filled with  $\text{SiO}_2$  ( $n_S = 1.46$ ), unless otherwise specified.

The E-field distribution across the structure shown in figure 1 can be seen in figure 2.a and 2.b for a slot-waveguide with silicon region width  $w_h = 180 \text{ nm}$ , slot width  $w_s = 50 \text{ nm}$ , and height  $h = 300 \text{ nm}$ . Figure 2.a shows the contours of the E-field amplitude and the E-field lines of the quasi-TE mode. The center bright region shows a strong E-field inside the slot. The directions of the E-field lines in the slot confirm that the total transverse E-field is mostly normal to the walls of the slot, which causes its discontinuity at the interface between silicon and slot. The E-field distribution can be seen more clearly in the 3D profile shown in figure 2.b. The peak amplitude of the E-field in the slot is 4 times higher than that in the silicon region, and 2.5 times higher than that in the cladding.

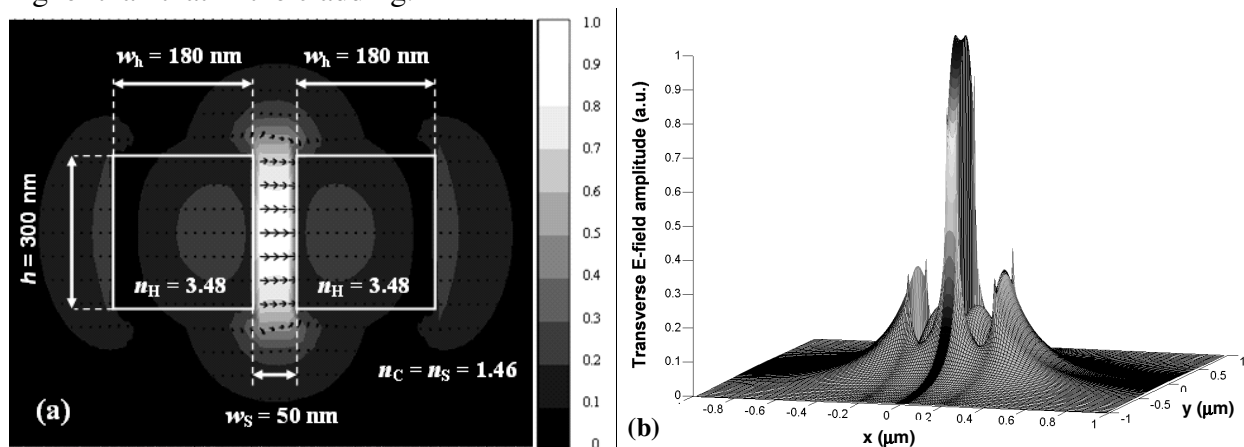


**Figure 2.** Transverse E-field profile of the quasi-TE mode. (a) E-field amplitude (contour) and lines. (b) 3D surface plot of the E-field amplitude. The origin of the coordinates system is located at the waveguide center; x-axis is horizontal direction and y-axis is vertical in part (a).

Figure 3.a shows the average optical intensity  $I_{\text{slot}}$  and the total optical power  $P_{\text{slot}} = h \cdot w_s \cdot I_{\text{slot}}$  in the slot as a function of  $w_s$  and  $w_h$  for  $h = 300 \text{ nm}$ . Both  $P_{\text{slot}}$  and  $I_{\text{slot}}$  are normalized with respect to the total optical power in the waveguide. For comparison, the normalized average optical intensity in the silicon region  $I_{\text{Si}}$  is plotted as well. The optical intensity is much higher in the slot than anywhere in the high-index region of the structure, which is a consequence of the E-field enhancement and the H-field invariance. Figure 3.a shows that  $P_{\text{slot}}$  remains nearly constant around 30% for  $w_s \geq 50 \text{ nm}$ . For  $w_s = 50 \text{ nm}$ ,  $I_{\text{slot}}$  is as high as  $20 \mu\text{m}^{-2}$ , which is 6 times higher than  $I_{\text{Si}}$ . One can also see from figure 3.a that  $w_h$  does not significantly affect the slot-waveguide performance.

In order to investigate the wavelength dependence, we simulated both  $P_{\text{slot}}$  and  $I_{\text{slot}}$  as a function of wavelength, as shown in figure 3.b. In the simulations, we used  $w_h = 180 \text{ nm}$ ,  $w_s = 50 \text{ nm}$ , and  $h = 300 \text{ nm}$ . The material dispersions have been taken into account in the simulations. One can see that the normalized power and intensity changed less than 10% over a wavelength

span of 400 nm. Therefore, the same slot-waveguide can be used to guide and confine light in a low-index material at a wide range of wavelengths, which greatly broadens its application scope.

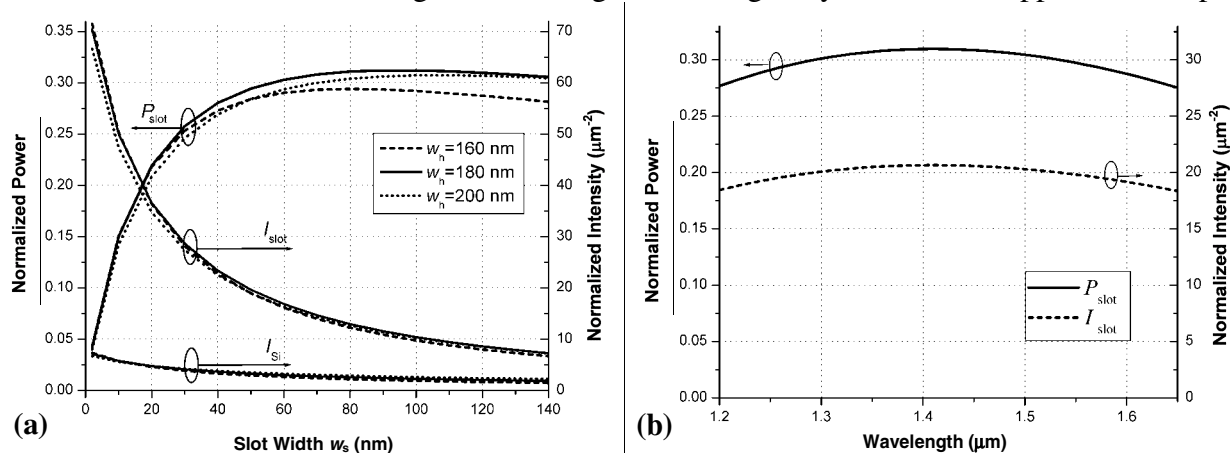


**Figure 3.** (a) Normalized power in the slot  $P_{\text{slot}}$ , normalized average intensity in the slot  $I_{\text{slot}}$ , and normalized average intensity in silicon  $I_{\text{Si}}$ , for quasi-TE mode in the slot-waveguide with  $\text{SiO}_2$  slot. Normalization is relative to the total optical waveguide power. (b) Normalized power  $P_{\text{slot}}$  and normalized average intensity  $I_{\text{slot}}$  in the slot as a function of the wavelength of light.

Light propagating in the slot waveguide not only is confined to a low-index material, but also has a much higher intensity than that achievable using conventional rectangular waveguides or photonic crystal waveguides. In order to numerically compare the performance of the slot waveguide with conventional rectangular SOI waveguides [1], we calculated the average intensity inside the core of the conventional SOI waveguide. When the cross-sectional dimension of the waveguide is large, the intensity is low because of the large mode size. When the dimension of the waveguide is too small, the intensity is also low because the mode becomes delocalized [10]. Therefore, there is an optimal waveguide dimension for achieving the highest intensity. The highest normalized average intensity in the core of the conventional SOI waveguide is less than  $9 \mu\text{m}^{-2}$ . Moreover, if the light is to be confined in a low-index material such as  $\text{SiO}_2$  with the conventional waveguide structure, the highest possible index contrast that can be achieved is through the  $\text{SiO}_2/\text{air}$  platform; the maximum normalized intensity that can be obtained in this case is less than  $1.1 \mu\text{m}^{-2}$ , which is almost 20 times lower than what we have calculated for the slot-waveguide. For the leaky-mode waveguides based on external reflections, such as the photonic crystal waveguide, the size of the low-index core is limited to be larger than half of the wavelength in the low-index material. Therefore, the normalized intensity can hardly exceed  $1 \mu\text{m}^{-2}$  at  $1.55\text{-}\mu\text{m}$  wavelength.

## EXPERIMENTS

We fabricated directional couplers (see figure 4.a) and ring resonators (see figure 4.b) with slot waveguides on a SOI platform using a process similar to that described in [10]. The waveguide dimensions are  $w_h = 220 \text{ nm}$ ,  $w_s = 100 \text{ nm}$ , and  $h = 250 \text{ nm}$ . From the directional couplers, the effective index can be extracted from the dependence of the coupling ratio on the lateral distance between adjacent slot-waveguides that form the directional coupler. From the ring resonator transmission spectra, the group index can be extracted from the free spectral range of their resonances.

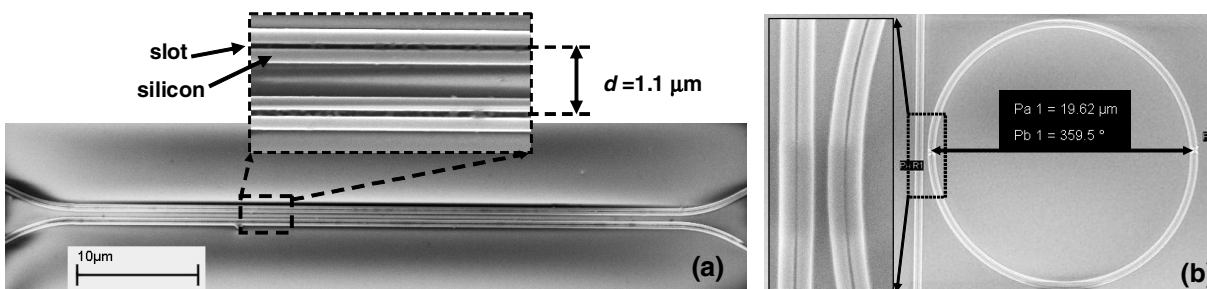


**Figure 4.** The top-view SEM picture of (a) a directional coupler and (b) a ring resonator, formed by two slot-waveguides fabricated using SOI platform.

The measured dispersion curves of the slot-waveguides that form the directional couplers are shown in figure 5.a, along with the ones obtained from simulations with actual device dimensions. Since the slots are found to be void, we used  $n_H = 3.48$ ,  $n_S = 1$ , and  $n_C = 1.46$ . The dispersion curve for a conventional waveguide, i.e.  $w_s = 0$ , are also calculated. The effective index of the quasi-TM mode is barely affected by the presence of the slot. In contrast, the effective index of the quasi-TE mode is drastically reduced due to the presence of the slot, what represents direct evidence that the power is indeed concentrated in the low-index region. The measured quasi-TE group index of the slot-waveguide that form the ring-resonator is shown in figure 5.b, along with the one obtained from simulations with actual device dimensions.

One can see from figures 5.a and 5.b that there is good agreement between theoretical predictions and experimental results, evidencing that the slot-waveguide is capable of strongly confining light in the low-index slot region and that it is compatible with highly-integrated photonics technology.

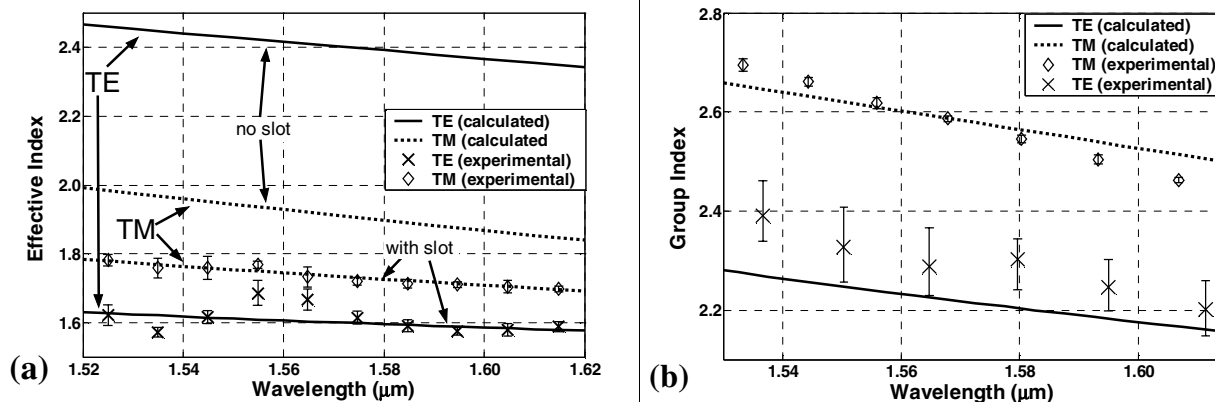


**Figure 5.** (a) Quasi-TE and quasi-TM modes; simulated (lines) and measured (marks with error bars) dispersion curves. Measurement was extracted from directional couplers with conventional and slot-waveguide ( $w_s = 0$ ). (b) Quasi-TE mode; simulated (lines) and measured (marks with error bars) group index. Measurement was extracted from ring resonators with slot-waveguides.

## CONCLUSIONS

In conclusion, we show experimental evidence that light can be efficiently guided and confined in low-index materials using E-field discontinuity in high-index-contrast material

systems. The slot-waveguide allows us to achieve high E-field amplitude and optical intensity in low-index materials at levels not attainable with conventional waveguides. This property enables highly efficient interaction between fields and active materials, which may lead to all-optical switch and parametric amplifier on Si integrated photonics. Since the E-field is strongly localized in a nanometer-sized low-index region, the slot-waveguide may be used to greatly increase the sensibility of optical sensing or to enhance the efficiency of near-field optical probes.

## ACKNOWLEDGEMENTS

The authors would like to thank Christina Manolatou for her guidance and assistance in the simulations. This work was supported by the Air Force Office of Scientific Research under grant number AFOSR F49620-03-1-0424. V. R. Almeida acknowledges sponsorship support provided by the Brazilian Defense Ministry. This work was performed in part at the Cornell Nano-Scale Science & Technology Facility (a member of the NNUN) which is supported by NSF under Grant ECS-9731293, its users, Cornell University and Industrial Affiliates. This work made use of the Cornell Center for Materials Research Shared Experimental Facilities, supported through the NSF MRSEC program (DMR-0079992).

## REFERENCES

1. K. K. Lee, D. R. Lim, L. C. Kimerling, J. Shin, and F. Cerrina, "Fabrication of ultralow-loss Si SiO<sub>2</sub> waveguides by roughness reduction," *Opt. Lett.* **26**, 1888 (2001).
2. A. Sakai, G. Hara, and T. Baba, "Sharply bent optical waveguide on silicon-on-insulator substrate," *Proceedings of SPIE* **4283**, 610 (2001).
3. C. Manolatou, S. G. Johnson, S. Fan, P. R. Villeneuve, H. A. Haus, and J. D. Joannopoulos, "High-density integrated optics," *J. Lightwave Technol.* **17**, 1682 (1999).
4. B. E. Little, J. S. Foresi, G. Steinmeyer, E. R. Thoen, S. T. Chu, H. A. Haus, E. P. Ippen, L. C. Kimerling, and W. Greene, "Ultra-compact Si-SiO<sub>2</sub> microring resonator optical channel dropping filters," *IEEE Photon. Technol. Lett.* **10**, 549 (1998).
5. M. A. Duguay, Y. Kokubun, and T. L. Koch, "Antiresonant reflecting optical waveguides in SiO<sub>2</sub>-Si multilayer structures," *Appl. Phys. Lett.* **49**, 13 (1986).
6. R. Bernini, S. Campopiano, L. Zeni, and C. de Boer, and P. M. Sarro, "Planar antiresonant reflecting optical waveguides as sensors for liquid substances," *Sensors, Proceedings of IEEE* **2**, 1160 (2002).
7. R. F. Cregan, B. J. Mangan, J. C. Knight, T. A. Birks, P. St. J. Russel, P. J. Roberts, and D. C. Allan, "Single-mode photonic band gap guidance of light in air," *Science* **285**, 1537 (1999).
8. S. G. Johnson, M. Ibanescu, M. Skorobogatiy, O. Weisberg, T. D. Engeness, M. Soljacic, S. A. Jacobs, J. D. Joannopoulos, and Y. Fink, "Low-loss asymptotically single-mode propagation in large-core OmniGuide fibers," *Optics Express* **9**, 748 (2001).
9. C. L. Xu, W. P. Huang, M. S. Stern, and S. K. Chaudhuri, "Full-vectorial mode calculations by finite difference method," *IEE Proc.-Optoelectron.* **141**, 281 (1994).
10. V. R. Almeida, R. R. Panepucci, and M. Lipson, "Nanotaper for compact mode conversion," *Opt. Lett.* **28**, 1302 (2003).